Real-Time FTIR and WAXS Studies of Drawing Behavior of Poly(ethylene terephthalate) Films

A. C. MIDDLETON,[1] R. A. DUCKETT,[1] I. M. WARD,[1] A. MAHENDRASINGAM,[2] C. MARTIN[2]

[1] IRC in Polymer Science & Technology, University of Leeds, Leeds LS2 9JT, United Kingdom

[2] Department of Physics, University of Keele, Keele, United Kingdom

Received 1 December 1999; accepted 24 April 2000

ABSTRACT: The development of molecular orientation and crystallization was studied during uniaxial drawing of poly(ethylene terephthalate) (PET) films, which was immediately followed by subsequent taut annealing at the drawing temperature. The behavior was monitored in real time throughout the drawing and annealing using dynamic FTIR spectroscopy and *in situ* WAXS measurements using the Daresbury Synchrotron Radiation Source. Films were drawn at 80 and 85°C at varying strain rates (0.001–0.7 s^{-1}). The true stress–strain behavior was determined at each of the drawing conditions and the density and optical anisotropy of unloaded samples was measured. The IR spectra were analyzed using curve reconstruction procedures developed previously, and they showed that orientation of the phenylene groups and the trans glycol conformers occurred before significant gauche–trans conformational changes could be seen. The onset of crystallization, defined as the point that the crystalline $\bar{1}05$ reflection could be first observed using WAXS, was not found to correlate with any specific change in the proportions of trans and gauche isomers nor with any feature on the stress–strain curve. However, it was clear that, for these comparatively low strain rates, crystallization occurred during the drawing process while the crosshead was moving and the draw ratio was increasing. The orientation of the crystallites was calculated from the $\bar{1}05$ reflection observed in a tilted film, transmission geometry. The crystallites were found to form at a draw ratio of about 2.5 with high orientation values ($P_2 > 0.8$) that increased during drawing and annealing to P_2 values of 0.95, irrespective of the drawing conditions. Semiquantitative measurements of crystallinity showed that the fraction of crystalline material that developed during drawing decreased with increasing strain rate. © 2001 John Wiley & Sons, Inc. J Appl Polym Sci 79: 1825–1837, 2001

Key words: FTIR; WAXS; drawing behavior; poly(ethylene terephthalate) (PET) films

INTRODUCTION

It has long been recognized that the changes in structure that occur on stretching poly(ethylene terephthalate) (PET) films are complex because they involve the simultaneous development of molecular orientation and crystallization. Considerable progress has been made by quantitative studies of the structure of the stretched films, notably by IR spectroscopy and X-ray diffraction. Until recently, however, our understanding has been severely limited by the fact that only the final stretched materials could be studied; it is clearly very desirable to understand how the structural changes occur during the deformation process.

Correspondence to: I. M. Ward (I.M.Ward@leeds.ac.uk).

Journal of Applied Polymer Science, Vol. 79, 1825–1837 (2001)

With the recent developments of FTIR and real-time X-ray diffraction measurements using a synchrotron radiation source, it is now possible to make quantitative structural measurements while stretching the sample and also to study the further development of crystallinity due to the annealing processes. These developments have provided the stimulus for the present research.

A useful starting point for an understanding of the mechanisms of deformation in PET is to consider the stretching of a molecular network.[1,2] IR studies have shown that the development of molecular orientation and the conformational changes that occur can be modeled in this way,[3] in spite of the observation that in many cases the final stretched samples show that significant crystallization has occurred.

In the research reported here these issues are explored in some detail by undertaking FTIR measurements and real-time X-ray diffraction measurements over a range of strain rates where crystallization occurs during the stretching process. It is shown that, rather surprisingly, the onset of crystallization is not reflected in any singular changes in the conformational content or the molecular orientation determined by IR spectroscopy.

EXPERIMENTAL

Sample Dimensions

Rectangular 11 × 4 mm samples were held between grips. Films of two different thicknesses were studied. The samples for the IR spectroscopy were 40 μm thick and were supplied by DuPont. These samples were also used in the WAXS experiments, but the majority of the WAXS studies were completed on 200 μm thick samples supplied by ICI Wilton.

Mechanical Measurements

The stress–strain behavior during drawing and annealing was studied by drawing samples in an Instron tensile testing machine. The load–extension curves were converted into plots of true stress versus strain using real-time draw ratio values measured from video recordings of the gross sample. The sample draw ratios did not increase linearly with crosshead displacement throughout the drawing period but instead progressed through two drawing regimes. At small crosshead displacements the draw increased approximately linearly with the crosshead movement, but at higher extensions the rate of increase of the draw ratio declined as the materials that were initially constrained between the clamps began to draw.

Birefringence Measurements

The birefringence of the samples after drawing, annealing, and quenching to ambient temperature was measured using a polarizing microscope with a rotary compensator. The primary reason for these measurements was to confirm that there were no significant differences in the structural changes occurring during drawing between samples of different thicknesses.

Density Measurements

The densities of samples used in the WAXS measurements were determined in a density column composed of aqueous potassium iodide. The measured samples had been drawn, taut annealed at the temperature of draw for 10 min and then quenched to ambient temperature.

IR Spectroscopy

Polarized IR spectra were recorded in real time by drawing samples in a Minimat materials tester mounted on the sample stage of a BOMEM MB-151 FTIR spectrometer. The spectrometer was controlled by an NEC personal computer using commercially available Spectra-Calc software. The chamber was heated by the circulation of hot air, and the glass entry and exit windows were replaced with potassium bromide (KBr). Parallel and perpendicular polarization spectra were recorded on successive samples that underwent identical thermal and mechanical histories. This could be justified because drawing under these conditions was found to be almost perfectly reproducible.

Figure 1 shows a schematic of the Minimat with the experimental arrangement required for the collection of polarized spectra while the sample is heated and drawn.

The maximum crosshead speed attainable using this rig was 99 mm/min; samples were drawn at 1, 5, 50, and 99 mm/min. These corresponded to nominal strain rates of 0.001–0.1 s^{-1}. The results from drawing at the three slow speeds allowed direct comparison with the WAXS experiments.

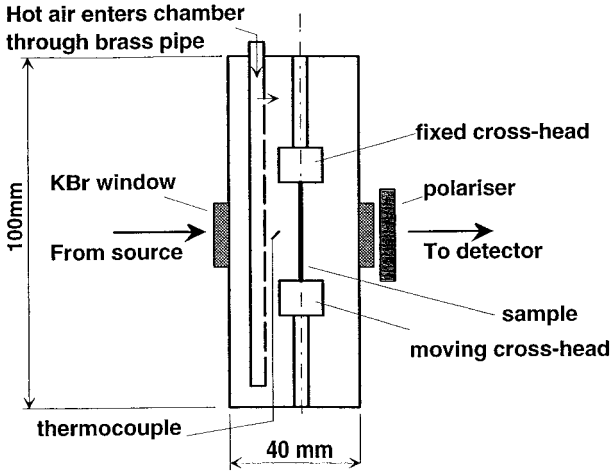

Figure 1 A schematic diagram of the temperature chamber for the Minimat material tester mounted on the BOMEM sample stage.

Spectra were collected with the sample in the isotropic state and throughout the drawing period for times up to 30 s after the crosshead stopped moving and after the sample had been annealed for 10 min. After the sample had been quenched, a final spectrum was recorded to allow any effects of the quenching to be studied.

When the samples were being drawn, a compromise had to be made between the speed with which the spectra could be obtained and their final quality. Details of the drawing conditions and the spectra collection times are given in Table I.

The frequency versus absorbance spectra were reconstructed into their constituent bands using a Fortran fitting program that uses the Nag library routine E04JAF to refine an initial guess of the spectrum by performing a least-squares minimization. Each spectrum was fitted with 36 Lorentzian peaks and a flat background in the 750–1020 cm^{-1} region. The peak heights, positions, and half-widths of all the bands used in the reconstruction were based on previously published values. The band assignments were also based on previous work, in particular that of Yazdanian and colleagues[4] who made special note of the different gauche and trans bands.

From our viewpoint the important band assignments relate to the benzene ring vibration bands at 873 and 878 cm^{-1}, which were used to determine the orientation of the phenylene units; the bands assigned to the trans glycol conformations at 972, 962, and 972 cm^{-1}; and those assigned to the gauche glycol conformations at 891, 899, and 906 cm^{-1}. These assignments are marked on the annotated spectrum shown in Figure 2.

Once the spectra had been resolved into their constituent peaks by curve fitting, the area under each Lorentzian curve was calculated. The volume of the sample intercepting the IR beam decreased with increasing draw ratio, and the spectra were normalized against the 794 cm^{-1} band to allow for the changing width and thickness of the samples. The nondichroic nature of the 794 cm^{-1} band meant that all band areas could be normalized to the area of the 794 cm^{-1} band for that particular spectrum without first correcting for dichroic effects.

The draw ratio corresponding to each spectrum was calculated from the change in the area of the 794 cm^{-1} band.

The unavoidable fact that the sample becomes narrower as the drawing proceeds means that an increasing proportion of the beam reaches the detector without passing through the sample. (It was impossible to significantly increase the initial width of the sample to avoid this without depart-

Table I Experimental Details of Dynamic IR Experiments

Temperature (°C)	Crosshead Speed (mm/min)	Time to Complete Draw (s)	Resolution (cm^{-1})	Scans Coadded/ Spectrum	Time to Collect Each Spectrum (s)
80	1	1800	2	20	100
80	5	360	2	5	25
80	50	100	2	1	5
80	99	18	2	1	5
85	1	1800	2	20	100
85	5	360	2	5	25
85	50	100	2	1	5
85	99	18	2	1	5

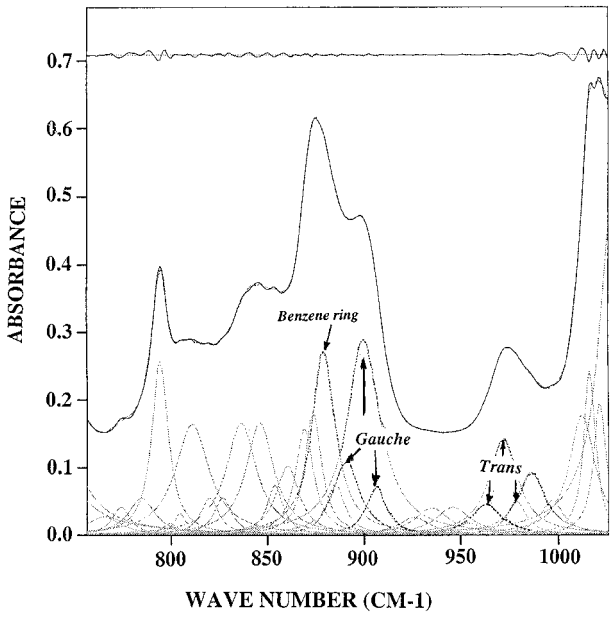

Figure 2 An IR spectrum of isotropic PET.

ing significantly from the desired uniaxiality of drawing.) This has the effect of changing the relative absorbencies of bands relating to trans and gauche conformation and reducing the apparent gauche/trans ratio. This effect causes the initial gauche content to be reduced from a true value of 80% (on the basis of previous research) to a value of 70%. The discrepancy increases with increasing draw ratio, so that the IR results should be regarded as semiquantitative.

The orientation values, $P_2(\theta_m)\langle P_2(\theta)\rangle_{\mathrm{IR}}$, of the trans (972 cm^{-1}) and gauche (891, 899, 906 cm^{-1}) conformers, and the benzene rings (873, 878 cm^{-1}) were calculated using the procedures described in previous articles.[5]

$$P_2(\theta_m)\langle P_2(\theta)\rangle_{\mathrm{IR}} = \frac{A_{\parallel} - A_{\perp}}{A_{\parallel} + 2A_{\perp}} \tag{1}$$

where $A_{\parallel}$ and $A_{\perp}$ are the absorptions with the polarization direction parallel and perpendicular to the draw direction, respectively; $P_2(\theta_m) = \frac{1}{2}(3\ \cos^2\theta_m - 1)$; θ_m is the fixed angle between the transition moment direction and the chain axis; $\langle P_2(\theta)\rangle = \frac{1}{2}\langle 3\ \cos^2\theta - 1\rangle$; and θ is the angle between a chain axis and the draw direction. The angle brackets indicate a mean value taken over all chain directions.

The 972 cm^{-1} band alone was used to indicate the trans orientation because the dichroism of the three trans bands is not identical: the 962 and 972 cm^{-1} bands have parallel dichroism while the 979 cm^{-1} is a perpendicular band.

The total trans conformer content was taken as the sum of the contents of the 963, 972, and 978 cm^{-1} bands. The total gauche conformer content ($\Sigma A_{0,\mathrm{gauche}}$) was taken as the sum of the 890, 899, and 906 cm^{-1} bands. The total content of each conformer could then be expressed as a percentage of the sum of the two quantities.

$$x_{\mathrm{trans}} = \frac{\sum A_{0,\mathrm{trans}}}{\sum A_{0,\mathrm{trans}} + \sum A_{0,\mathrm{gauche}}} \tag{2}$$

where $\Sigma A_{0,\mathrm{trans}} = A_{\parallel\mathrm{trans}} + 2A_{\perp\mathrm{trans}}$, and so forth.

WAXS Measurements

In this study the weak but clearly distinguishable $\bar{1}05$ reflection was used to quantitatively monitor the development of crystallinity.

Theoretical

The crystalline $\bar{1}05$ reflection is the closest reflection to the meridian in the PET diffraction pattern. The $\bar{1}05$ plane normals make an angle of approximately 10° with the crystal c axis.[6] In order to place the diffraction peak of the reflection exactly on the Ewald sphere, it is necessary to incline the specimen at an angle of θ_{hkl}, the Bragg angle for the reflection. The Bragg angle for the $\bar{1}05$ reflection is ~21° for the wavelength of radiation produced at the Daresbury Synchrotron Radiation Source (SRS), and so the sample must be tilted through this angle if accurate orientation information is to be recorded from this reflection.

If a sample is tilted to bring the reciprocal lattice point onto the sphere of diffraction and a flat plate is then used to record the diffraction pattern, the "azimuthal" angle that is measured on the diffraction pattern has to be corrected using the following equation to allow for the tilt[7,8]:

$$\cos\ \phi = \sin^2\phi_{hkl} + \sin\ \alpha\ \cos^2\phi_{hkl} \tag{3}$$

where ϕ is the corrected azimuthal angle and α is the "azimuthal" angle on the experimental diffraction pattern, which is measured from the equator.

If defining the chain axis direction rather than the plane normal corresponding to the $\bar{1}05$ reflection is desired, it is necessary to make a further correction, as discussed by Auriemma et al.[6] To a

very good approximation the angle ϕ between the c axis and the draw direction is given by

$$\cos^2\phi = \cos^2\phi \cos^2\gamma$$

where γ is the angle between the normal to the $\bar{1}05$ plane and the c axis.

In this case $\gamma \sim 10°$, so that $\cos^2\gamma \sim 0.97$. In view of the comparatively broad $\bar{1}05$ reflection, we did not consider it appropriate to make this correction but rather to quote the results in terms of the orientation of the $\bar{1}05$ plane normals.

Experimental

The samples studied using WAXS were drawn in an X-ray camera built for this purpose.[9,10] The camera was heated by two heating elements, and the air was circulated by wall mounted fans. The camera was mounted on its side and positioned so that the sample was tilted through an angle of 21° toward the incident beam. The instrumentation required to perform dynamic experiments and collect diffraction patterns in real time using the Keele camera is discussed fully in Blundell et al.[11]

All the real-time WAXS experiments were carried out at the Daresbury SRS. The beam had a monochromated wavelength of 1.488 Å, and the current varied from 156 to 131 mA during each 24-h period.

The diffraction pattern was collected using a CCD camera. The camera was placed normal to the incident X-ray beam and close to the aluminum foil window in order to reduce air scatter to a minimum. Unfortunately the size of the detector area and the geometry of the experiment meant that only part of the pattern was recorded. The detector was therefore carefully positioned so that it was able to record both the center of the diffraction pattern and the $\bar{1}05$ reflection.

Each specimen was marked with dots at 1-mm intervals along its length prior to drawing. A video camera was mounted outside the drawing camera and focused on the sample through the glass side wall. The gross appearance of the sample during drawing and annealing was recorded, and this allowed the diffraction pattern to be related to the corresponding state of deformation of the sample at any time.

Experiments were performed on single thicknesses of the thick film samples and on four thicknesses of the thin film samples sandwiched together within the grips.

Table II Collection Time for Each Diffraction Pattern during Real-Time WAXS Experiments

Drawing Speed (mm/min)	Collection Time (s) During	
	Draw	Annealing
1	10	10
5	10	10
50	10	10
500	0.4	10 (from video tape)

Diffraction patterns were recorded during three stages of the experiment: prior to the draw when the sample had reached the drawing temperature, throughout the draw, and throughout the annealing period.

The length of time taken to acquire each diffraction pattern was dependent upon the time taken to complete the draw. Experiments in which the crosshead moved at 500 mm/min took less than 4 s to complete, and so each diffraction pattern was the result of adding only 10 frames (1 frame = 40 ms). A diffraction pattern was therefore recorded every 400 ms during the draw. Further details are given in Table II.

Analysis

Diffraction patterns were recorded using a Photonic Science CCD detector with a sensitive area of 92 × 69 mm.[12] Each pixel on the detector had an effective area of 120 × 120 μm and was capable of recording intensities over the range of 0–64,000. Diffraction patterns were recorded on the CCD detector with exposure times of 40 ms. During this time the pattern was accumulated within the detector before being digitized by a Synoptic I860 frame grabber within an 8-bit word binary data format. The signal to noise ratio was improved by integrating successive frames together, and the number of frames depended on the time taken to complete the experiment.

After collection, the files were downloaded through a SCSI interface to a PC. In parallel with the transfer of data to the frame grabber, the signal accumulated in the CCD during each 40 ms was written to a standard video cassette recorder using a VHS format. (Each frame on the video cassette also corresponded to 40 ms.) This served as a backup of the raw data and also allowed the files to be reanalyzed, integrating over different numbers of frames, if that was later thought to be advantageous.

Each diffraction pattern was analyzed using the data analysis package VIEWX.

The development of orientation was followed by analyzing an azimuthal circular scan across the $\bar{1}05$ reflection of each frame. The scan covered the longest arc possible on the diffraction pattern; but this was only 60° of the whole azimuth, which was centered on the meridian, rather than one whole quadrant of the diffraction pattern, which would have been ideal.

The noncrystalline contribution to be removed from the intensity recorded on the reflection was calculated by linear interpolation between the azimuthal scans on either side of the $\bar{1}05$ reflection. In most cases the background scans were approximately linear.

The scans were then corrected for the tilt of the film to produce plots of intensity versus the genuine azimuthal angle using eq. (3) above.

These plots were fitted to Gaussian curve profiles as shown in Figure 3, and values for the Hermans' orientation function $P_{2(\bar{1}05,M)}$ were calculated using the equations

$$\langle \cos^2 \phi_{(105,M)} \rangle = \frac{\sum_0^{90} I(\phi) \cos^2 \phi \sin \phi}{\sum_0^{90} I(\phi) \sin \phi} \quad (4)$$

and

$$P_{2(105,M)} = \frac{1}{2}(3\langle \cos^2 \phi_{(105),M} \rangle - 1) \quad (5)$$

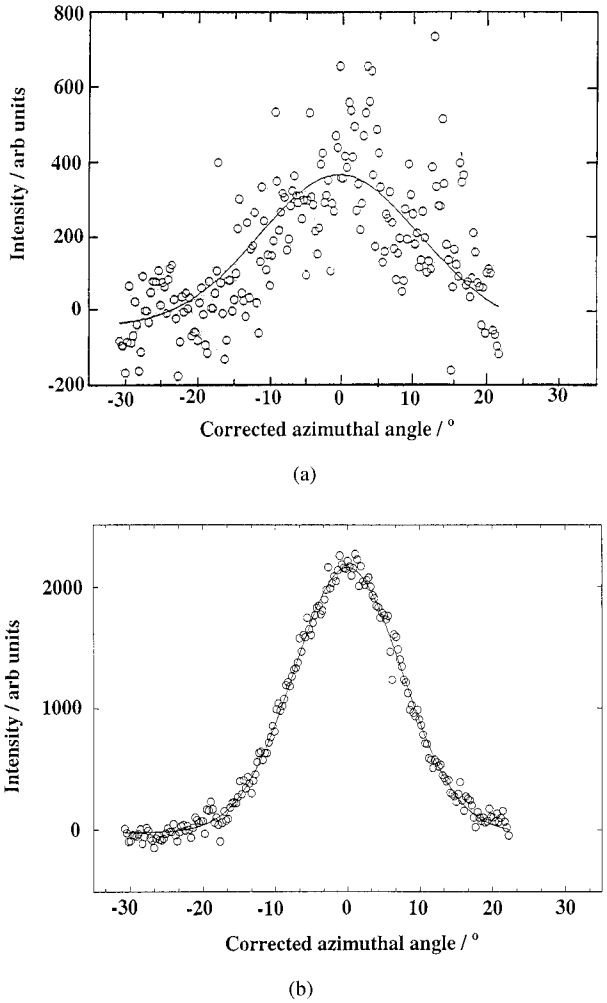

Figure 3 (a) A Gaussian curve fitted to corrected data from a typical diffraction pattern recorded when the $\bar{1}05$ reflection was just visible: (○) data points and (—) a fitted Gaussian. (b) A Gaussian curve fitted to corrected data from a typical diffraction pattern recorded when the $\bar{1}05$ reflection was well established: (○) data points and (—) a fitted Gaussian.

RESULTS

Birefringence Measurements

The birefringences of each of the samples are plotted against the crosshead speed in Figure 4. The thin IR sample drawn at 85°C only attained a draw ratio of 3.0 and hence should not be considered in the following discussion.

The lowest levels of orientation were shown by the samples drawn at 85°C and 1 mm/min and the highest levels were displayed by the samples stretched at 80°C and 500 mm/min. The birefringence at first changed rapidly with increasing crosshead speed in the range of 1–5 mm/min. The rate of increase then dropped for crosshead speeds of 50–500 mm/min.

These results are replotted with the crosshead speed on a logarithmic scale in Figure 5. The relationship is approximately linear.

The two graphs both indicate that it is the temperature of drawing, rather than the film thickness, that differentiates samples drawn at any one crosshead speed from each other. Samples drawn at 80°C always had greater birefringence values relative to those drawn at 85°C, whether they were drawn from thin or thick film. The results from both films at either temperature are in fact indistinguishable from each other. This

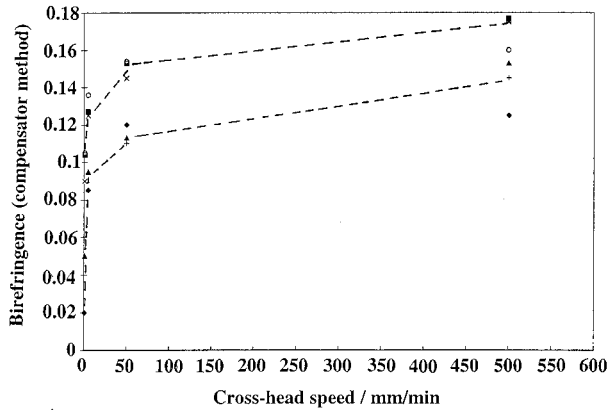

Figure 4 The final birefringence vs the crosshead speed for samples studied in real time using WAXS and IR spectroscopy: (■) 80°C thick WAXS; (▲) 85°C thick WAXS, (×) 80°C thin WAXS, (+) 85°C thin WAXS, (○) 80°C thin IR, and (◆) 85°C thin IR.

reinforces the premise that results from samples of different thicknesses can be usefully compared.

Density Measurements

The results of the density measurements performed on the dynamic WAXS samples are plotted against the crosshead speed in Figure 6. Each sample had a draw ratio of close to 3.6. The density first increased steeply with the crosshead speed and then increased more slowly for speeds greater than 50 mm/min. The lowest density values, which were recorded for the thick samples drawn at 85°C and 1 mm/min, implied that the material had not begun to crystallize. The density was close to that assumed for isotropic amorphous PET and had an identical value to that of the starting material. In contrast, the highest density value, which was attained for the thick sample drawn at 500 mm/min and 80°C, implied a mass fraction crystallinity of approximately 23%.

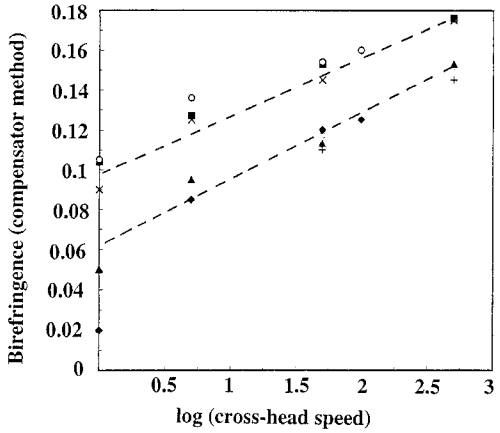

Figure 5 The relationship between the birefringence and crosshead speed (plotted on a logarithmic scale) for dynamic samples studied using WAXS and IR spectroscopy: (■) 80°C thick WAXS, (▲) 85°C thick WAXS, (×) 80°C thin WAXS, (+) 85°C thin WAXS, (○) 80°C thin IR, and (◆) 85°C thin IR.

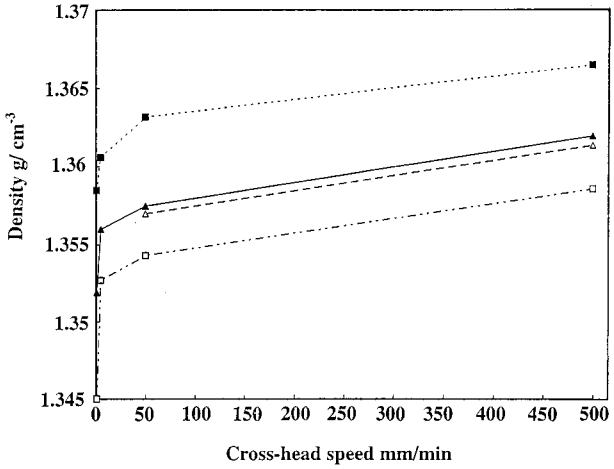

Figure 6 The variation in density with the crosshead speed for thin and thick WAXS samples drawn to a draw ratio of 3.6 at 80 and 85°C and annealed for 10 min: (■) 80°C thick, (▲) 80°C thin, (□) 85°C thick, and (△) 85°C thin.

IR Spectroscopy

Figure 7(a,b) shows the variation in the trans and gauche conformer contents and the orientation of the trans, gauche, and benzene ring bands, respectively, for samples drawn at 80°C and a crosshead speed of 5 mm/min. Similar results for a crosshead speed of 50 mm/min and 80°C are shown in Figure 8(a,b). It should be noted that the dotted lines are included purely as visual aids to emphasize the trends in the data.

Summary of Measurement of Trans and Gauche Conformers

The isotropic, amorphous film was composed of 68(±1)% gauche conformers and 32(±1)% trans conformers. As discussed above, these numbers are systematically low because the sample does not cover the beam.

The conversion of the gauche conformers into the trans conformation did not begin as soon as the draw ratio started to increase. Instead the

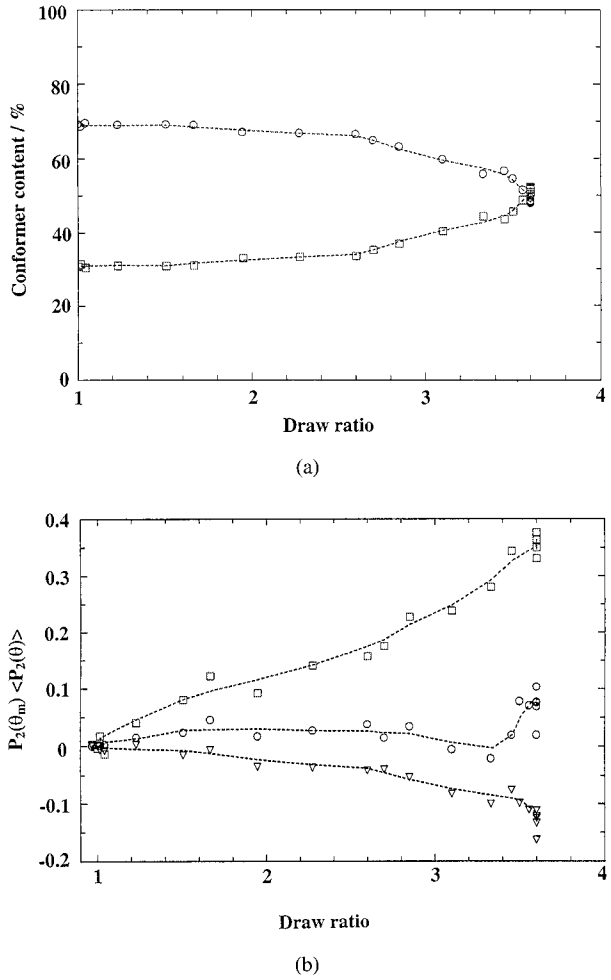

Figure 7 The (□) trans and (○) gauche contents as functions of the draw ratio for a sample drawn at 80°C and 5 mm/min. (b) The orientation of (□) 975 cm^{-1} trans, (○) 890 + 899 + 906 cm^{-1} gauche, and (▽) 872 + 878 cm^{-1} benzene ring bands as functions of the draw ratio for a sample drawn at 80°C and 5 mm/min.

trans/gauche content remained approximately constant at first and only started to change when the draw ratio had passed a value of at least 2. It is difficult to identify the exact draw ratio at which the conversion process begins; but the draw ratio at which a marked change was first observed seemed to decrease as the drawing speed increased, being close to a draw ratio of 3 for the samples drawn at 1 and 5 mm/min but closer to 2 for samples drawn at the faster rates. There was no obvious change in this trend with the temperature of drawing.

The majority of the gauche to trans conversion occurred while the crosshead was moving, but there were also some changes during the annealing period while the draw ratio remained constant. It should be noted that the possible variations in the conformer contents at the final draw ratio appeared to be artificially high on these graphs because random scatter in the data would have the same appearance as a genuine trend when all the data points are plotted at the same draw ratio.

There were no systematic differences between the spectra recorded while the samples were being annealed and those recorded after the quench. This implies that once the sample was annealed for 10 min at the temperature of draw, the structure was not further affected by the quenching process and did not undergo any further changes in the time required to achieve the quench.

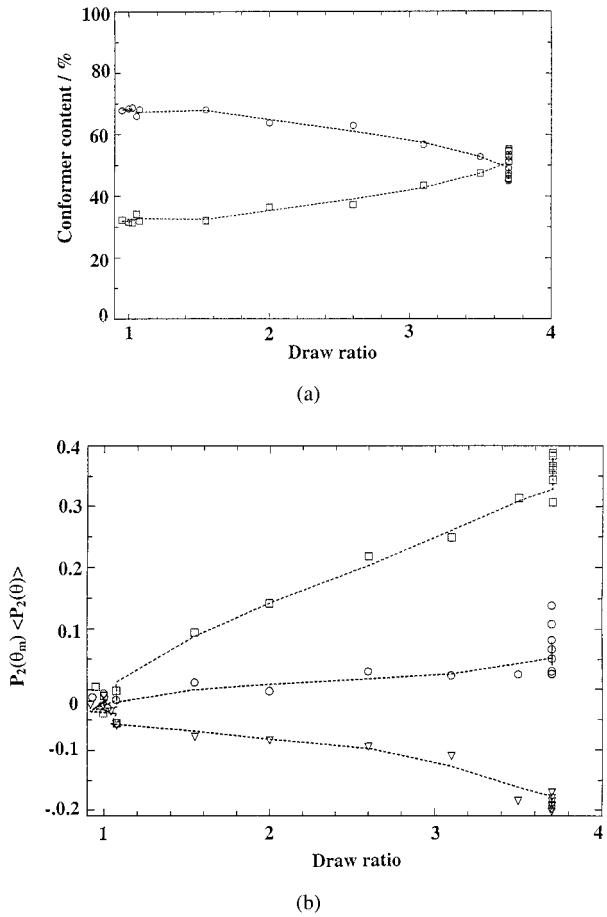

Figure 8 (a) The (□) trans and (○) gauche contents as functions of the draw ratio for a sample drawn at 80°C and 50 mm/min. (b) The orientation of (□) 975 cm^{-1} trans, (○) 890 + 899 + 906 cm^{-1} gauche, and (▽) 872 + 878 cm^{-1} benzene ring bands as functions of the draw ratio for a sample drawn at 80°C and 50 mm/min.

Observations on IR Orientation Measurements

Orientation of the 972 cm^{-1} trans band occurred very early in the draw, well before the conversion of gauche to trans began.

The final degree of orientation of the trans bands was lower for all samples drawn at 85°C than for any samples drawn at 80°C.

There was no obvious trend in the final degree of orientation of the trans bands with the drawing speed, but some trends could be identified in the *rate* at which the orientation progressed. Samples drawn at the faster rates showed appreciable orientation at lower draw ratios compared to those drawn at slow rates. This trend was particularly noticeable in the samples drawn at 85°C, the $P_2(\theta_m)\langle P_2(\theta)\rangle_{IR}$ having a value of 0.15 at a draw ratio of 2 for the sample drawn at 99 mm/min, compared to a value of 0.05 at the same draw ratio for the experiment completed at 5 mm/min.

The orientation of the 890, 899, and 906 cm^{-1} gauche bands was always very low and could be approximated to zero within experimental error.

Orientation of the 872 and 878 cm^{-1} benzene ring bands was first observed early in the draw at approximately the same time as the orientation of the 973 cm^{-1} bands.

In contrast to the behavior of the trans bands, the orientation of the benzene ring bands showed some variation with both the drawing speed and temperature. Drawing at 80°C induced a higher degree of orientation than drawing at 85°C at each drawing speed, with the exception that samples drawn at the fastest speeds at 85°C reached levels of orientation similar to samples drawn slowly at 80°C.

There did not seem to be any sudden changes in the trans/gauche ratio that could relate to the onset of crystallization.

WAXS Study

The progression of the crystallization of each sample was monitored by recording the peak intensity of the reflection and comparing it with the draw ratio at that time. The crystallinity is actually related to the integrated area under the reflection, but because the Gaussian half-width of the reflection underwent very little change during the course of each experiment, a semiquantitative study can be completed by simply considering the peak intensity.

Figure 9 shows the development of the crystalline $\bar{1}05$ peak for samples drawn at 5 mm/min.

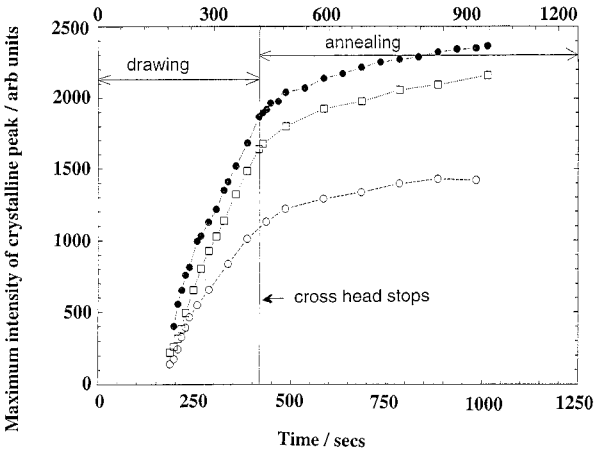

Figure 9 The development of the crystalline peak during drawing and annealing of samples drawn at 5 mm/min: (●) 80°C thin, (□) 80°C thick, and (○) 85°C thick.

Crystallization clearly occurred during the draw. Once it reached a recordable level, the peak intensity of the azimuthal scan then increased approximately linearly throughout the remainder of the draw. It may be that the development of the crystalline reflection proceeded smoothly from zero, in which case the peak may have existed in earlier diffraction patterns without rising clear of the noise. Alternatively, the peak behavior may be as presented here, such that the peak initially shows discontinuous growth. This would agree with the hypothesis of other researchers that crystallization is initiated from many different centers as soon as a critical condition is established (e.g., the amorphous orientation passes a certain level).[13,14]

Draw ratios at which the reflection first became apparent during each experiment were always close to 2.5, and it was difficult to discern any other trend from the data.

Figure 10 shows the variation of the orientation parameter $\langle P_2(\theta)\rangle_{\bar{1}05,m}$ and the true stress values with the draw ratio for the 200-μm sample drawn at 80°C and 5 mm/min. (The orientation parameter is abbreviated to P_2 in the figures.) The point at which a Gaussian curve can first be fitted to the WAXS data does not seem to correspond to any particular feature on the true stress–strain curve, and the majority of the draws under all conditions showed a similar lack of correlation between the onset of crystallization and the true stress versus strain.

The orientation of the $\bar{1}05$ crystallites is always very high, appearing with values of 0.80 to

0.90 and rising to 0.95 by the end of the annealing period, regardless of the drawing conditions. It is difficult to identify the first diffraction pattern at which the peak became discernible from the background noise level, and obviously if any scans were to show the broader peaks indicative of lower orientation it would be these early scans. However, none of the recorded data fitted Gaussian curves with larger half-widths and the conclusion that the average orientation of the crystallites is always very high would seem to be justified. The majority of the increase in orientation occurred during the draw, but there was also a perceptible rise during the annealing period.

Figure 11 compares the relative growths of the peak intensity during drawing and annealing for samples drawn at different speeds. The fraction of the crystalline peak that develops during the draw is expressed as a percentage of the final peak intensity recorded after 10-min annealing. In the slowest draws, the peak attains a value close to the final value while the crosshead is moving. In contrast, during the fastest draws, less than half of the maximum peak intensity is attained while the crosshead is moving. Instead the majority of the crystallization occurs during the annealing period. The data lie on a straight line when time is plotted on a logarithmic scale; if this behavior is extrapolated to higher drawing speeds, it implies that a crosshead speed of 1×10^6 mm/min would be required for all the crystallization to occur during the annealing period rather than during the draw. The fastest high speed spinning rates are currently 6000 m/min for cold drawing (i.e., 6×10^6 mm/min).

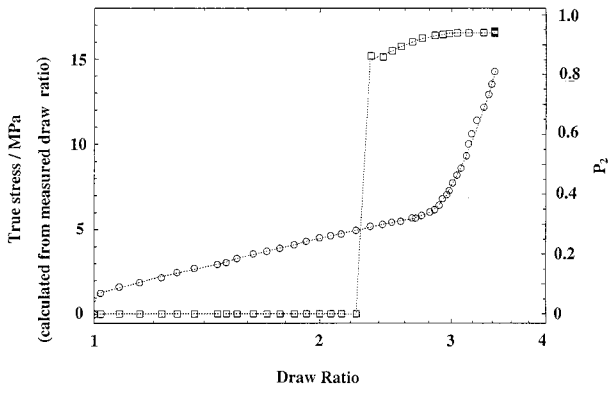

Figure 10 The (□) P_2 and (○) true stress vs the draw ratio for thick samples drawn at 80°C and 5 mm/min.

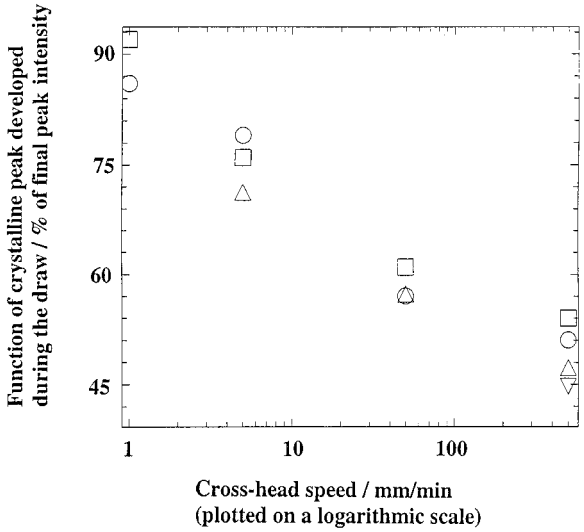

Figure 11 The fraction of the crystalline peak developed during the draw expressed as a percentage of the final peak intensity: (□) 80°C thick, (○) 80°C thin, (△) 85°C thick, and (▽) 85°C thin.

DISCUSSION

Crystallization during Draw

The most significant conclusion that can be drawn from the real-time WAXS results is that the crystallization occurs while the crosshead is moving and the draw ratio is increasing. This is further confirmation of recent results by Blundell et al.[12] The crystalline peak was first observed for draw ratios close to 2.5, and no clear trend emerged from the data between the draw ratio and the temperature or speed of drawing. However, the fraction of the final intensity that developed while the crosshead was moving showed a definite correlation with the drawing speed and implied that drawing at very high speeds would result in crystalline reflections that developed entirely after the crosshead stopped moving. The time that elapsed between the start of the draw and the appearance of the crystalline reflection varied enormously with the drawing speed. Samples drawn at 500 mm/min showed evidence of crystallization after 1–3 s whereas samples drawn at 1 mm/min did not crystallize until nearly 1000 s had elapsed. There is clearly then no simple correlation between crystallization and time for the results presented here.

The polymer research group at the University of Keele worked in collaboration with ICI to investigate the orientation and crystallization be-

havior of PET film in real time during high speed drawing. Their early results[11,12,15] from high speed drawing showed that significant crystallization *does not* begin until the conclusion of drawing. They used the Keele camera and data collection methods similar to the ones described in this work but studied the equatorial reflections in the normal transmission geometry. Isotropic, amorphous PET films were drawn at temperatures in the 80–110°C range and draw ratios close to 4. The experiments were performed at the European Synchrotron Radiation Facility, and very fast strain rates of approximately 10 s^{-1} were used. The high intensity of the Microfocus beamline meant that diffraction patterns could be recorded every 40 ms. In each of the experiments there was a hint of the crystalline reflections superimposed on the diffuse equatorial spots, and therefore a possibility that the very beginnings of crystallization occurred just before the final draw ratio was achieved. However, it was clear that the major intensification of the crystalline reflection occurred in subsequent frames after drawing had stopped. In Blundell et al.'s most recent work[16] they confirm that crystallization does occur during drawing at low rates and propose that a unified treatment of the effects of time and temperature can be achieved using a WLF time–temperature shift factor.

Interrupted drawing experiments have historically been taken to imply that the crystallization occurs while the crosshead is moving. For example, Kaito et al.[17] drew samples at 80°C and found crystallization began to increase from draw ratios of approximately 2.5. Several studies found that the draw ratio of the onset of crystallization actually *decreases* with increasing draw rate, although it should be noted that the range of draw ratios observed was quite narrow.[13,14,17–19] Jabarin[19] further states that when stretching occurs at high speeds to high draw ratios, all the strain induced crystallization occurs during the draw and there are no further changes during annealing.

Crystallite Orientation

The main conclusion that can be drawn from the WAXS orientation studies in this work is that the crystallite orientation is always very high. Crystallites must therefore be formed from highly oriented chain segments rather than from unoriented regions that rotate toward the draw direction at a later stage. No trend could be identified that related the exact value of the orientation function to the drawing conditions.

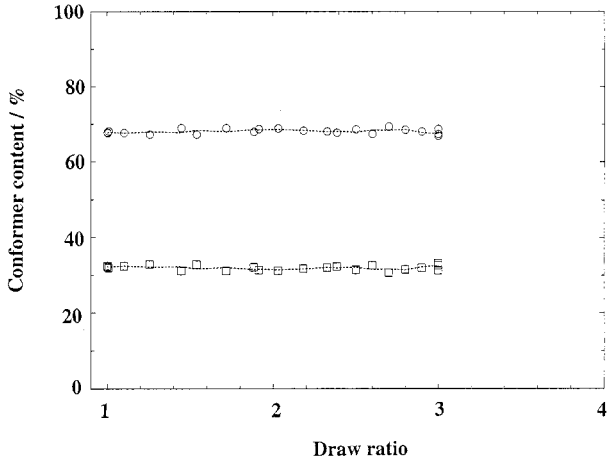

Figure 12 The (□) trans and (○) gauche conformer content as a function of the draw ratio for a sample drawn at 85°C and 1 mm/min.

The near-perfect orientation of the crystallites in drawn PET samples was noted in many "interrupted drawing" studies (i.e., measurements on samples after drawing, cooling, and unloading). Padibjo and Ward[20] measured crystallite orientation values and found they were always greater than 0.90. Göschel et al.[21] drew film at 80°C and measured the crystallite orientation to be 0.98 from the equatorial WAXS reflections. Kaito et al.[17] found the crystallite orientation function increased from 0.7 to 0.8 during drawing and reached a final value of 0.95 after annealing.

It was not possible to correlate the onset of crystallization with any particular feature of the true stress–strain curve for the drawing conditions studied in this work. However, samples drawn at all rates showed that crystallization began below the onset of rapid strain hardening.

A comparison of the results from the real-time WAXS and IR experiments suggests that the onset of crystallization detected by WAXS does not relate to any marked change in the gauche/trans isomerism behavior. If the draw ratios for the onset of crystallization from the WAXS results are related to the IR results, then it can be seen that significant gauche/trans isomerization does not always occur before evidence of crystallization is detected in the WAXS pattern. Figure 12 gives no evidence of gauche/trans isomerization at any stage of the draw, even though the WAXS experiments show that crystallization occurs under these drawing conditions. Crystallization in this

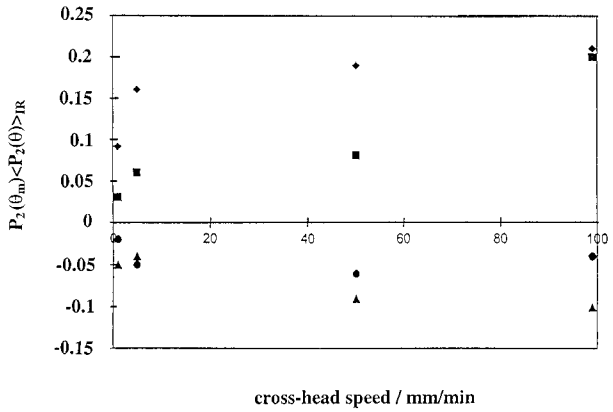

Figure 13 The orientation of (□) 975 cm^{-1} trans and (▽) 872 + 878 cm^{-1} benzene ring bands at the draw ratio of crystallization measured from the WAXS results: (◆) 80°C trans, (■) 85°C trans, (▲) 80°C benzene, and (●) 85°C benzene.

case must initiate between trans molecules that existed in the starting material.

The orientation of the IR bands at the draw ratio corresponding to the onset of crystallization in the WAXS results is shown in Figure 13, which plots the orientation function as a function of the crosshead speed. Two trends can be identified from the graph: the value of $P_2(\theta_m)\langle P_2(\theta)\rangle_{\text{trans}}$ increases with increasing crosshead speed and the orientation level is greater for drawing at 80°C than for drawing at 85°C. The benzene ring results are not as clear but seem to show the same trend. This trend was unexpected because the work of Le Bourvellec et al.[22] found that there was a critical orientation of the trans amorphous chains required for the initiation of crystallization. The critical level depended on the temperature of stretching (decreasing with increasing temperature) but not the strain rate. Hirahata et al.[23] explained the dependence on temperature in the following way: the lower the temperature, the lower the mobility of the chains and the more the chains must be oriented to compensate for this low mobility. A larger number of amorphous trans chains are then required, which contributes to the formation of stable nuclei.

All the trans bands must be "amorphous" trans before the onset of crystallization, and so the results presented here imply that their critical orientation increases with both the temperature and strain rate. For these results to agree with those of Le Bourvellec et al.,[22] there must be a time delay between the point at which the IR results register the critical orientation and the point when the onset of crystallization is detectable in the WAXS results. The change in the draw ratio during this time delay would obviously be greatest for samples drawn at the fastest strain rates. This would then lead to a graph with the form shown in Figure 13. This time delay could possibly arise because crystallization must occur on a larger scale to be measurable by WAXS than to be measurable by IR experiments because it describes the orientation of much larger assemblies. Also, Hirahata et al.[23] suggested that the orientation need not be uniform throughout the material, so that even when the average orientation (as measured by WAXS or birefringence) is low, a small part of the chains, in the regions where the entanglements of the chains are more stable, may become highly oriented. These chains can then act as crystal nuclei.

The finding that the average orientation of the crystallites continues to increase during annealing is of some interest. Possible explanations for this can be suggested. Either the crystallites that have already formed must continue to orient during annealing or the crystallites that form during annealing must originate from amorphous material with near-perfect orientation. Because the crystallinity was shown to increase during annealing, the number of the crystallites must increase. Heffelfinger and Schmidt[24] postulated that crystallization occurs by one of two methods: transformation of oriented gauche material into crystalline trans or conversion of amorphous trans into crystalline trans. The IR results in this work show that the conversion of gauche to trans continues into the annealing stage of the processing, which would indicate a major contribution from the former process. However, the IR results also show no evidence of orientation in the gauche conformers at any stage. Crystallization during annealing by this route alone would therefore be expected to lower the mean crystallite orientation unless the gauche conformers convert into highly oriented trans conformers in an energetically favorable process. Crystallization during taut annealing seems likely to occur predominantly in the oriented trans regions and must mainly involve the formation of load-bearing (972 cm^{-1}) crystallites because the non-load-bearing (962 cm^{-1}) bands show no significant growth during this period. The true explanation of the effects that were observed is most likely to be a combination of the possibilities suggested above.

CONCLUSIONS

The combination of FTIR spectroscopy and WAXS results taken during the drawing and taught annealing of PET film provided considerable insight into the mechanism of drawing and crystallization. Gauche/trans isomerization was clearly detectable during drawing at a rate that increased with an increasing draw rate and decreasing temperature. The orientation of the trans conformers also increased in a similar way. The WAXS technique is sensitive only to those trans conformers in the crystalline regions, and these were only detected at draw ratios above approximately 2.2. When observed, the crystallites were highly oriented, more oriented than the overall trans orientation. The onset of crystallization as detected by WAXS was not marked by any sudden change in number or orientation of the trans conformers nor with any particular feature of the stress–strain curves. There is clear evidence that crystallization occurs during the drawing process, although at the higher drawing speeds the majority of the crystallization observed occurred during the taut-annealing process.

A. C. Middleton held an EPSRC CASE studentship sponsored by ICI Films. The authors thank Dr. D. J. Blundell and Dr. D. MacKerron of ICI Films for their contributions to this research.

REFERENCES

1. Rietsch, F.; Duckett, R. A.; Ward, I. M. Polymer 1979, 20, 1133.
2. Long, S. D.; Ward, I. M. J Polym Sci Polym Phys Ed 1991, 42, 1921.
3. Lapersonne, P.; Bower, D. I.; Ward, I. M. Polymer 1992, 33, 1277.
4. Yazdanian, M.; Ward, I. M.; Brody, H. Polymer 1985, 26, 1779.
5. Cunningham, A.; Ward, I. M.; Willis, H. A.; Zichy, V. Polymer 1974, 15, 749.
6. Auriemma, F.; Guerra, G.; Parravicini, L.; Petraccone, V.; Russo, G. J Polym Sci Part B: Polym Phys 1995, 33, 1917.
7. Bacon, G. E. J Appl Chem 1956, 6, 477.
8. Gupta, V. B.; Ramesh, C.; Patil, N. B.; Chimdambareswaran, P. K. J Polym Sci Polym Phys Ed 1983, 21, 2425.
9. Mahendrasingam, A.; MacKerron, D. H.; Fuller, W.; Forsyth, V. T.; Oldman, R. J.; Blundell, D. J. Rev Sci Instrum 1992, 63, 1097.
10. Blundell, D. J.; Mahendrasingam, A.; MacKerron, D.; Turner, A.; Rule, R.; Oldman, R. J.; Fuller, W. Polymer 1994, 35, 3875.
11. Blundell, D. J.; MacKerron, D. H.; Fuller, W.; Mahendrasingam, A.; Martin, C.; Oldman, R. J.; Rule, R. J.; Riekel, C. Polymer 1996, 37, 3303.
12. Fuller, W.; Mahendrasingam, A.; Martin, C.; Hughes, D. J.; Oatway, W.; Heeley, E. In Proceedings of the 30th International Symposium on Novelties in Textiles; 1996.
13. Salem, D. R. Polymer 1992, 33, 3189.
14. Salem, D. R. Polymer 1992, 33, 3182.
15. Mahendrasingam, A.; Martin, C.; Jaber, A.; Hughes, D. J.; Fuller, W.; Rule, R. J. Nucl Instrum Methods Phys Res 1995, B97, 238.
16. Blundell, D. J.; Oldman, R. J.; Fuller, W.; Mahendrasingam, A.; Martin, C.; MacKerron, D.; Harvie, J. M.; Riekel, C. Polym Bull 1999, 42, 357.
17. Kaito, A.; Makayama, K.; Kanetsuna, H. J Polym Sci Polym Phys Ed 1988, 26, 1439.
18. Ajji, A.; Guèvremont, J.; Cole, K. C.; Dumoulin, M. M. Polymer 1996, 37, 3707.
19. Jabarin, S. A. Polym Eng Sci 1992, 32, 1341.
20. Padibjo, S. R.; Ward, I. M. Polymer 1983, 24, 1103.
21. Göschel, U.; Deutscher, K.; Abetz, U. Polymer 1996, 37, 1.
22. Le Bourvellec, G.; Monnerie, L.; Jarry, J. P. Polymer 1986, 27, 856.
23. Hirahata, H.; Seifert, S.; Zachmann, H. G.; Yabuki, K. Polymer 1996, 37, 5131.
24. Heffelfinger, C. H.; Schmidt, P. G. J Appl Polym Sci 1965, 9, 2661.